Tunneling into Superconductors at Temperatures below 1°K

I. Giaever, H. R. Hart, Jr., and K. Megerle

General Electric Research Laboratory, Schenectady, New York

The density of states in four superconductors, lead, tin, indium, and aluminum, has been studied using the tunneling technique. The experimental results agree remarkably well with the Bardeen-Cooper-Schrieffer theory; however, two exceptions were found. The energy gap is not as sharp in the experiment as in the theory, but this may merely be due to imperfect samples. The density of states in lead has definite but small divergences from the theory.

INTRODUCTION

A CENTRAL part in the Bardeen-Cooper-Schrieffer[1] theory of superconductivity is the creation of an energy gap in the electron density of states when a metal is made superconducting. Experimental evidence for this gap can be obtained by several different methods,[2] and a particularly illustrative and simple one is electron tunneling.[3-6] In a tunneling experiment the sample consists of a thin insulating layer sandwiched between two evaporated metal films. Experimentally, the electron tunneling current through the insulating layer is observed as a function of voltage applied between the two metal films. By using the tunneling technique one obtains not only the magnitude of the energy gap, but also the corresponding density of states.

Previous experiments[7] have been done only in the temperature range $T > 1°K$, but in this range kT is still an appreciable fraction of the energy gap and results in a temperature smearing. We decided to repeat some of the experiments at a lower temperature $T \geqslant 0.3°K$ by using a helium-three refrigerator. Also, to give the Bardeen-Cooper-Schrieffer theory a closer check, it was decided to measure the slope of the current-voltage curve (dV/dI or dynamic resistance) directly, as it is this quantity which is inversely proportional to the density of states. Tin, lead, indium, and aluminum were the superconductors studied.

ELECTRICAL APPARATUS AND MEASURING CIRCUITS

The resistance plotter measures the dynamic resistance of the tunnel junction as a function of junction current. This measurement is accomplished by superimposing a small alternating current of constant amplitude on the bias current through the junction and observing the ac voltage developed across the junction. Since the nonlinear resistance characteristics of the junction occur over the range of a few millivolts, great care must be taken to obtain high resolution and accuracy. The resistance plotter is schematically shown in Fig. 1. The circuit used to observe the small 8-cps voltage appearing across the junction is essentially a high-gain synchronous detector which has the required high signal-to-noise ratio.

To measure the ac voltage appearing across the junction, a modified Beckman (model 14) 8-cps breaker amplifier is used.[8] The modifications to the Beckman amplifier consist of removal of the breakers and breaker drive assembly and direct connection of the input to the input transformer. The breakers and drive assembly are located outside the amplifier and are connected to it by shielded cables.

The breaker drive mechanism also synchronously drives an electromechanical 8-cps generator. This generator consists of a small permanent magnet rotating in the polegap of a pickup coil. The phase between the 8-cps generator and breakers can be varied through 360° by rotating the pickup coil relative to the generating magnet.

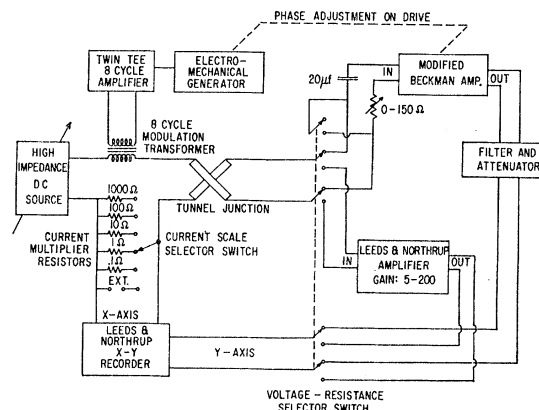The 8-cps signal from the pickup coil is fed to a twin-tee amplifier for wave-shaping and amplitude

Fig. 1. Schematic drawing of the electrical measuring circuit. The resistance plotter is essentially a high-gain synchronous detector with a high signal-to-noise ratio.

[1] J. Bardeen, L. N. Cooper, and J. R. Schrieffer, Phys. Rev. **108**, 1175 (1957).

[2] M. A. Biondi, A. T. Forrester, M. P. Garfunkel, and C. B. Satterthwaite, Revs. Modern Phys. **30**, 1109 (1958).

[3] I. Giaever, Phys. Rev. Letters **5**, 147 (1960).

[4] J. Nicol, S. Shapiro, and P. H. Smith, Phys. Rev. Letters **5**, 461 (1960).

[5] I. Giaever, Phys. Rev. Letters **5**, 464 (1960).

[6] I. Giaever and K. Megerle, Phys. Rev. **122**, 1101 (1961).

[7] *Note added in proof*. N. V. Zavaritskii, J. Exptl. Theoret. Phys. (U.S.S.R.) **41**, 657 (1961), and Soviet Phys.—JETP **14**, 467 (1962), has done experiments with the same superconductors down to 0.1°K.

[8] M. D. Liston, C. E. Zuinn, W. E. Sargeant, and G. G. Scott, Rev. Sci. Instr. **17**, 19 (1946).
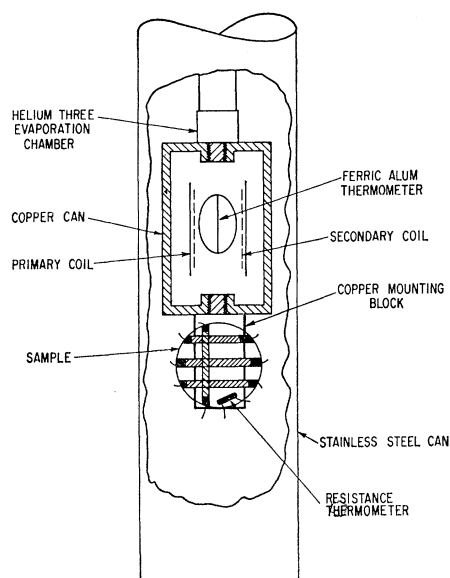
FIG. 2. Schematic detail of the helium-three refrigerator showing sample, sample mounting, and thermometry.

control and then drives a modulation transformer. The modulation transformer applies the 8-cps signal to a series circuit consisting of the junction, the current multiplier resistors used to measure the junction current, and a high-impedance dc source used to bias the junction. For high resolution, the 8-cps signal amplitude appearing across the junction is of the order of one microvolt or less.

The 8-cps voltage appearing across the junction is fed through a blocking capacitor and a variable-impedance matching resistor directly to the input transformer of the modified Beckman amplifier. After amplification, the 8-cps signal is converted to dc by the output breakers of the Beckman amplifier. This dc voltage is then passed through filter and attenuator networks and applied to the Y axis of a Leeds and Northrup $X-Y$ recorder. The X axis of this recorder simultaneously measures the junction current. A continuous plot of resistance vs current is obtained through the use of a motor driven output control in the dc bias source. The bias current through the junction must change slowly to allow the synchronous detector to follow changes in the sample resistance.

To insure accuracy, the resistance plotter is always calibrated over the required range of resistance values. Calibration is effected by replacing the junction and junction leads with an equivalent circuit of known resistances. Nonlinearity in the resistance plotter is chiefly due to phase shift and impedance mismatch in the input circuit of the Beckman amplifier. The effect of phase shift is small and can be minimized by adjusting the phase of the 8-cps generator relative to the output breaker of the Beckman amplifier. Nonlinearity due to impedance mismatch at the Beckman amplifier input

is also small if the load seen by the amplifier input transformer is within a factor of 3 of its nominal design impedance. The linear range has been extended further by using either one half or the entire primary winding of the input transformer depending on the range of resistances to be measured. Nonlinearity due to amplifier distortion does not occur since the input signal is always small.

In the course of the experiments, it was noted that in some cases the voltage vs current and resistance vs current plots were not reproducible. The trouble was traced to 60-cps ac noise across the junction. This ac noise was introduced by ground loops between the X-Y recorder and the various amplifiers. By proper selection of grounding points and polarity, the ac noise appearing across the junction was reduced to less than 5 μv peak-to-peak as measured with an oscilloscope. As a final check, an I-V curve taken with the automatic recording instruments was compared with an I-V curve from the same sample obtained with a completely shielded potentiometer and ammeter measuring circuit. The agreement was excellent, indicating that most of the ac noise had been eliminated.

CYROGENIC APPARATUS

For the experiments between 0.3° and 1.2°K the sample was mounted in a helium-three refrigerator typical of those described in the review article by Taconis.[9] As shown in Fig. 2, the helium-three evaporation chamber served as a cold finger to which were attached a paramagnetic salt thermometer and a copper block which contained a carbon-resistance thermometer. The sample, a sapphire single crystal supporting three tunneling junctions and a carbon-film resistance thermometer, was glued to the copper block. The above assembly was mounted in a vacuum chamber formed by the stainless steel can which was closed with an indium O-ring seal. In early experiments a Woods Metal joint was used but it was found that the heat and flux damaged the thin film samples.

In order to limit the heat input to the sample, the electrical leads within the refrigerator were made of 0.0076-cm diameter Manganin wire tinned with a lead-tin solder, superconducting at these temperatures. The leads were thermally attached to a heat sink at about 1.15°K and then to the helium-three evaporation chamber before going to the sample.

The paramagnetic-salt thermometer consisted of a 28 cps mutual-inductance bridge with an elliptical sample of ferric ammonium alum formed from two single crystals.[10] The thermometer, including the niobium primary coil and the secondary coil, was

---

[9] K. W. Taconis, *Progress in Low-Temperature Physics*, edited by C. J. Gorter (North-Holland Publishing Company, Amsterdam, 1961), Vol. III, Chap. V.
[10] D. deKlerk, in *Handbuch der Physik*, edited by S. Flügge (Springer-Verlag, Berlin, 1956), Vol. 15, pp. 154, 71.

mounted in a thick-walled can made of OFHC copper. The necessary thermal contact was established by many fine insulated copper wires. The inside of the can was tinned with a superconducting solder to eliminate eddy currents,[11] and to prevent errors in thermometry due to magnetic materials outside the can. The salt thermometer was calibrated against the helium-four vapor pressure using the 1958 scale.[12] The magnetic temperatures were converted to absolute temperatures using the data of Cooke, Meyer, and Wolf.[13] The temperature uncertainty at 0.30°K is about ±0.01°K.

The sample film resistance thermometers were formed by painting onto the sapphire crystal a thin film of Microcircuits Company RS-12 Shielding Micropaint. The two carbon-resistance thermometers were calibrated against the paramagnetic salt in the absence of any power input to the tunneling junctions.

In the initial experiments the sapphire crystal was glued directly to the copper block with Apiezon N vacuum grease. It was found that there was a tendency for the bond between the cold grease and the crystal to shear. Dow-Corning DC-200, 20 000 cs, silicon fluid was superior to the vacuum grease but shearing still occurred. The problem was met by gluing with GE-7031 low-temperature varnish,[14] a single layer of 0.0063-cm diameter Formex coated copper wires to the copper block, and then gluing the crystal to the copper wires with the 20 000 cs silicon fluid. The tunneling junction resistances were chosen high enough to allow the helium-three refrigerator, including the above glued joints, to maintain the desired temperatures during a run. The temperature of the sapphire crystal could be monitored during the run with the film resistance thermometer.

SAMPLE PREPARATION

The samples consist of two metal films separated by a thin insulating layer. Metal/metal-oxide/metal sandwiches were prepared by vapor depositing a suitable metal strip onto a single-crystal sapphire substrate, oxidizing the surface of this metal layer in the atmosphere, and then vapor-depositing three cross strips of a second metal over the insulating oxide film. Metals used to form insulating oxide films were magnesium, lead, tin, and aluminum. A more detailed description of sample preparation is given in previous publications.[6,15] Single crystal sapphire was used as a substrate for these experiments to obtain good thermal contact between the metal films and the helium three refrigerator.

MODEL

The tunneling experiment can be explained qualitatively using very simple models,[6] and quantitative calculations can be made using the Bardeen-Cooper-Schrieffer theory. The interpretation of the experiment hinges on the assumption that the transition probability is proportional to the density of states in a superconductor, an assumption shown to be plausible by Bardeen.[16] Harrison[17] has shown that, while the transition probability is not proportional to the density of states in a normal metal, it is still a function of the density of states. It is, therefore, puzzling that no results indicating a varying density of states in a normal metal have been seen experimentally in spite of several attempts, in particular using nickel.

With the assumption that the transition probability is proportional to the density of states in superconductors, one obtains for the current:

$$I = C_{NN} \int_{-\infty}^{\infty} \rho_1(E)\rho_2(E+eV)[F(E)-F(E+eV)]dE, \quad (1)$$

where C_{NN} is the conductance when both metals are normal, ρ_1 and ρ_2 are the ratios between the superconducting and normal densities of states in the two metal films, F is the Fermi function, e is the electronic charge, and V is the applied voltage.

In this report we are interested particularly in the tunneling between a normal and a superconducting member. For $T=0$ we obtain from (1):

$$[dI/dV]_{NS}=0, \quad eV < \epsilon$$

$$[dI/dV]_{NS}=C_{NN}\left\{\frac{eV}{(eV)^2-\epsilon^2}\right\}^{\frac{1}{2}}, \quad eV > \epsilon; \quad (2)$$
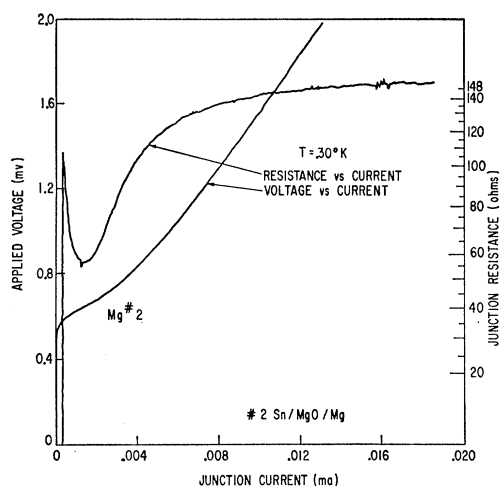

FIG. 3. Photographic reproduction of experimental curves obtained from a Sn−MgO−Mg tunnel junction showing voltage vs current and resistance vs current.

[11] G. Seidel and P. H. Keesom, Rev. Sci. Instr. **29**, 606 (1958).
[12] F. G. Brickwedde, Physica **24**, 5128 (1958).
[13] A. H. Cooke, H. Meyer, and W. P. Wolf, Proc. Roy. Soc. (London) **A233**, 536 (1956).
[14] J. C. Wheatley, D. F. Griffing, and T. L. Estle, Rev. Sci. Instr. **27**, 1070 (1956).
[15] J. C. Fisher and I. Giaever, J. Appl. Phys. **32**, 172 (1961).

[16] J. Bardeen, Phys. Rev. Letters **6**, 57 (1961).
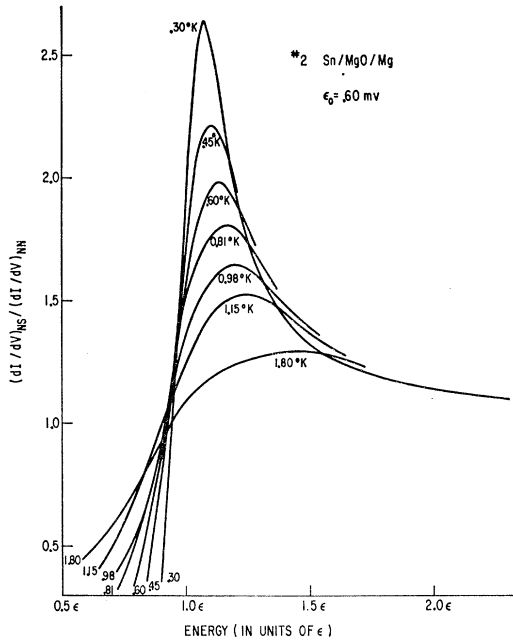[17] W. A. Harrison, Phys. Rev. **123**, 85 (1961).

FIG. 4. The relative conductance of a Sn—MgO—Mg sandwich; i.e., the conductance of the sandwich when the tin film is superconducting, divided by the conductance when the tin film is normal, plotted against energy normalized to the energy gap for several different temperatures. Since the energy gap is a function of temperature, we have used the experimentally verified BCS variation of the gap with temperature for the energy normalization. The energy gap at $T=0$ is given in the figure. Note that for maximum detail the zero has been offset.

i.e., the relative conductance $(dI/dV)_{NS}$ is directly proportional to the density of states.

Due to the logarithmic infinity in the density of states, one gets appreciable kT smearing when $eV \sim \epsilon$ even at low temperatures. In order to test the theory in this region, one can study two superconductors with equal energy gaps. At $T=0$ one obtains

$$I_{SS}=0, \quad eV<2\epsilon$$

$$I_{SS}=C_{NN}\left[\frac{(eV)^2}{2\epsilon+eV}K\left(\frac{eV-2\epsilon}{eV+2\epsilon}\right)+(eV+2\epsilon)\right. \tag{3}$$

$$\left. \times\left\{E\left(\frac{eV-2\epsilon}{eV+2\epsilon}\right)-K\left(\frac{eV-2\epsilon}{eV+2\epsilon}\right)\right\}\right], \quad eV>2\epsilon,$$

where K and E are complete elliptic integrals. It is not difficult to see from (1) that kT smearing is of much less importance in this case, and in particular that there is a discontinuous jump in current at $eV=2\epsilon$ even at finite temperatures.

EXPERIMENTAL RESULTS

We have studied four different superconductors at low temperatures; namely, tin, lead, indium, and aluminum. Since we studied tin most extensively, we shall report on this in some detail as the typical sample,

pointing out differences with other samples as they occur.

(a). Tin

In Fig. 3 the results of a typical run on a Sn-MgO-Mg sandwich are shown. Voltage vs current and resistance vs current are plotted on the same graph to correlate resistance with applied voltage. In Fig. 4, we show the relative conductance as a function of energy, normalized to the measured energy gap, for a number of different temperatures. The normalized curves are very dependent upon the energy gap used, and it is difficult to determine the energy gap from the experimental curves of normal-insulator-superconductor sandwiches to closer than ±3%. In Fig. 5 we compare experimental and calculated curves of relative conductance vs normalized energy for a Sn-MgO-Mg sandwich at two different temperatures. By comparing the steeply rising portion of calculated and experimental curves, at energies slightly less than ϵ, it is apparent that only one value of ϵ will give a good fit. The value of ϵ used to normalize the energy scale of the figures is the value obtained from tunneling between two superconductors. From Fig. 5 it is also apparent that the experimentally-observed maximum conductance is less than the calculated value. We believe that this is due to a smearing of the energy gap.

A possible source of error is that we do not have an ideal four-probe measurement because the magnesium
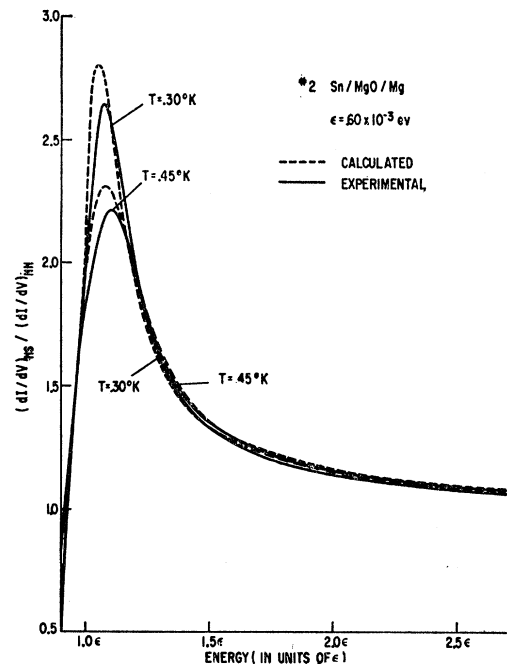

FIG. 5. Comparison of experimental and calculated relative conductance curves plotted against normalized energy for two different temperatures. The BCS density of states was used in the calculations. Note that for maximum detail the zero has been offset.
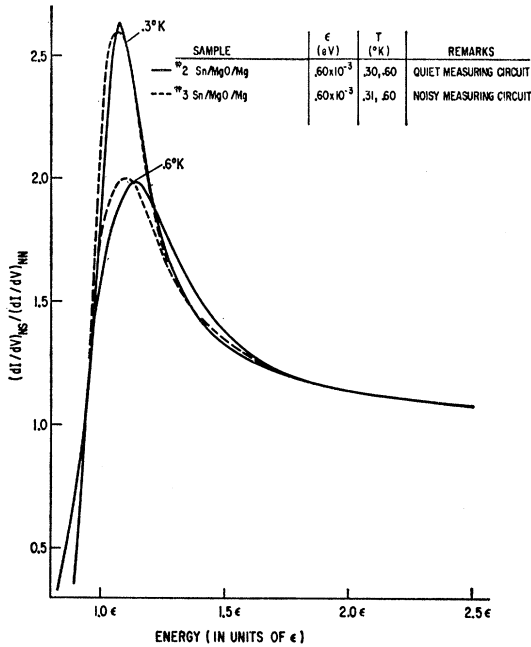
FIG. 6. Comparison of the relative conductance vs energy curves at two temperatures and taken from two different samples. There is a slight broadening of the curves obtained from the earlier run (No. 3). This broadening was due to induced ac noise in the measuring circuit. Note that for maximum detail the zero has been offset.

input to the helium-three refrigerator and to better match the impedance of the resistance plotter. Because of the low temperature, the leakage current tended to dominate the tunnel current at applied voltages less than half the gap width $(eV < \epsilon)$, and therefore the typical sample could not be used for temperature measurements. However since the leakage current in the experiments reported on always was less than $1/1000$ of the normal tunneling current, it has no significant effect on our results.

As seen from the curves it is not possible, within the errors of the experiment, to point to any large divergence between the Bardeen-Cooper-Schrieffer theory and the experimental results. However the edge of the energy gap is still badly smeared in spite of the low temperature. By using two superconductors, in this case Sn-SnO$_x$-Sn, and by taking extreme care in eliminating noise one finds a small divergence from the Bardeen-Cooper-Schrieffer theory; the jump in current at $eV = 2\epsilon$ is missing. In Fig. 8 the experimental results are shown together with a curve calculated from the Bardeen-Cooper-Schrieffer theory. We have chosen to use for the gap width the energy at which the current starts increasing rapidly with voltage. This is a somewhat arbitrary choice and in Fig. 9 we see the results of an attempt to obtain better agreement between theory and experiment by introducing into the Bardeen-
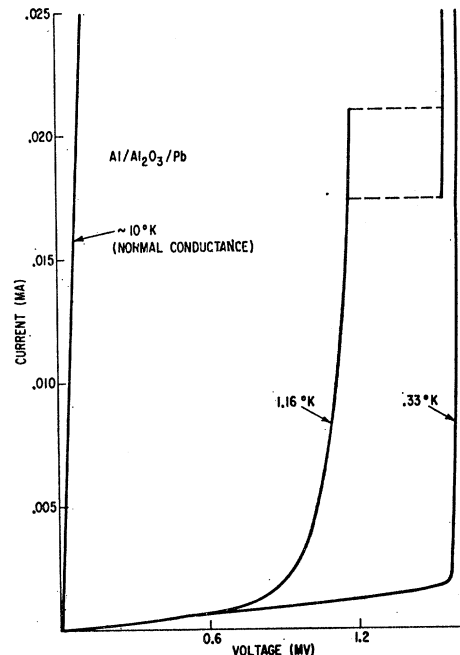
strip has resistance. By assuming an ideal sample geometry, having a strip resistance per unit length of R_s and a dynamic tunneling resistance per unit area of R_F, the error in measurement is

$$\frac{[dV/dI]_{NS}}{R_F} = \frac{(R_s/R_F)^{\frac{1}{2}}}{\sinh(R_s/R_F)^{\frac{1}{2}}}.$$

For the particular tin sample shown $R_s/R_F \sim 0.01$, when R_F is taken as the normal tunneling resistance, thus the error is of the order of less than $\frac{1}{2}\%$. To minimize this error we use the asymtotic resistance as the normalizing resistance.

Induced ac noise was a constant source of worry and it undoubtedly smeared the results. In Fig. 6 is shown a plot of two different runs; the earlier one having more noise and a less favorable (R_s/R_F) ratio. As seen, the scattering is small.

Another problem is caused by leakage current through the oxide. When a small leakage current is present, it will dominate the tunnel current for $kT \ll \epsilon$. A typical illustration of this effect is given in Fig. 7. Our experience has been that the lower we make the sample resistance (thinner oxide), the better the sample behaves. The reason is probably that the tunnel current increases much faster than the leakage current when the oxide thickness is reduced. The sample resistance in this case was chosen quite high, approximately 5 ohms for the 1-mm^2 junction, to minimize the heat

FIG. 7. Current-voltage characteristic for a Pb-Al$_2$O$_3$-Al sandwich showing the effect of leakage current. In this case the normal tunneling current dominates the leakage current, the ratio is approximately 1000:1. At 1.16°K the leakage current dominates at low voltages, $eV \ll \epsilon$. At 0.33°K the leakage current dominates for $eV \leqslant \epsilon$, and even wipes out the negative resistance effect. The leakage current appears to be ohmic and temperature insensitive as compared to the tunneling current.
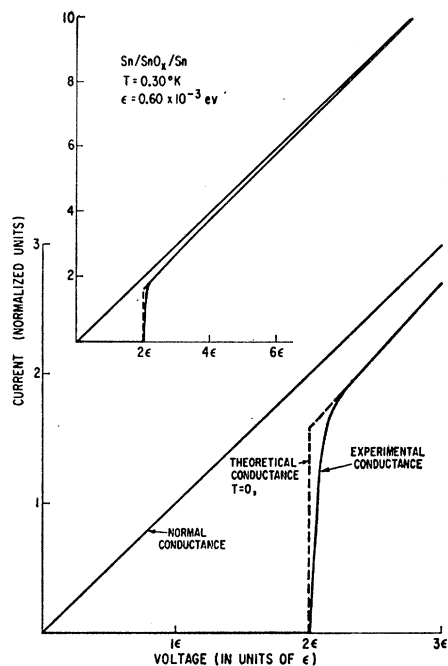
FIG. 8. Current voltage characteristic for a Sn-SnO$_x$-Sn sandwich. For comparison we show a calculated curve using the pure BCS density of states. Note that the experimental curve does not have the current jump one finds from the BCS theory.

Cooper-Schrieffer theory an energy breadth or smearing as done by Hebel and Slichter.[18] In this case the gap width 2ϵ and the smearing $2\epsilon\delta$ were chosen by visual curve fitting. Though the Hebel-Slichter smearing introduces the finite slope observed in the experimental data, the experimental curve does not have the rounded knee for low current values. The insert on Fig. 9 shows a detailed picture of this; note that the experimental curve is dominated by a leakage current for the lower current values. Thus probably no significance can be attached to the observed rounding. Also, by getting the better fit in the voltage range approximately equal to 2ϵ, the experimental and calculated curves tend to disagree slightly for larger voltages, though it may be argued that the fit is still within the experimental accuracy. Thus, because the origin of the finite slope is unclear, we have chosen the energy gap to be the value at which current first appears.

Several reasons can be thought of for this nonideal behavior. The most likely cause is a smearing of the gap due to a nonuniform strain across the sample. As will be seen below in the study of aluminum, films having different thicknesses have different energy gaps and different transition temperatures, presumably because of the effects of strains due to the difference in thermal expansion between the film and the substrate.

If one attributes the smearing to lifetime one finds a

lower limit of 10^{-11} sec. Anisotropy of the energy gap is a likely reason, but the smearing is much less than the anisotropy obtained from ultrasonic measurements.[19] This result indicates that Anderson's theory of a dirty superconductor applies quite well to these films.[20] It is interesting to note that in tin[21] and lead[22] the smearing is of the same order of magnitude as the isotope effect; thus we are worried about a rather small effect. Of course, it may be that the Bardeen-Cooper-Schrieffer approximation of a constant interaction potential, made in order to be able to handle the integral equation analytically, does not apply too well in the region of the gap.

(b). Lead

In Fig. 10 the density of states obtained for a Pb-MgO-Mg sample is shown. Again a striking resemblance with the theory is found, except for the bumps in the density of states at higher energies. The bumps may be accounted for by having an energy-gap parameter ϵ_k which is *not* a constant. Thus

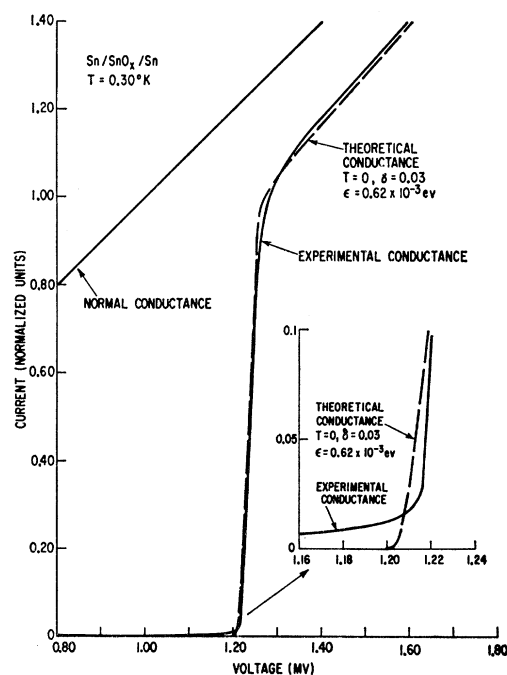$$E_k = [\eta_k{}^2 + \epsilon_k{}^2]^{\frac{1}{2}},$$

FIG. 9. Current voltage characteristic for a Sn-SnO$_x$-Sn sandwich. For comparison we show a calculated curve using the smeared BCS density of states of Hebel and Slichter. Note that for maximum detail the zero has been offset and an expanded view of the low-current region is shown.

[18] L. C. Hebel and C. P. Slichter, Phys. Rev. **113**, 1504 (1961).

[19] R. W. Morse, T. Olsen, and J. D. Gavenda, Phys. Rev. Letters **3**, 15 (1959).
[20] P. W. Anderson, J. Phys. Chem. Solids **11**, 26 (1959).
[21] E. Maxwell, Phys. Rev. **78**, 477 (1950).
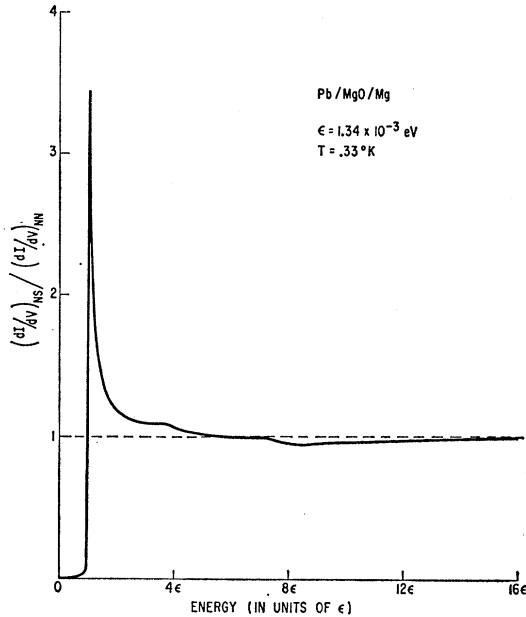[22] C. A. Reynolds, B. Serin, W. H. Wright, and L. B. Nesbitt, Phys. Rev. **78**, 487 (1950).

FIG. 10. The relative conductance of a Pb-MgO-Mg sandwich plotted against energy. At higher energies there are definite divergences from the BCS density of states as can be seen from the bumps in the experimental curve. Note that the crossover point corresponds in energy to the Debye temperature.

where E_k is the total energy and η_k is the single-particle energy. For an isotropic superconductor, ϵ can be written as a function of η only and the density of states
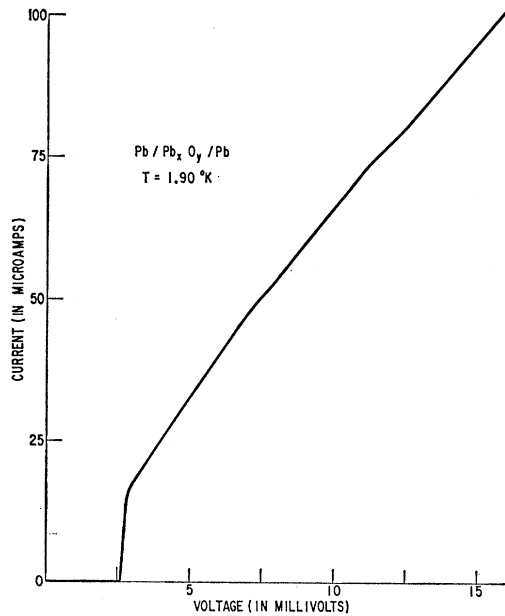

FIG. 11. Current vs voltage curve for a Pb-Pb$_x$O$_y$-Pb sandwich. At $eV \simeq 2\epsilon$ the current rises with a finite slope, rather than the jump in current predicted by the Bardeen-Cooper-Schrieffer theory. At applied voltages approximately equal to 6 mv and 11 mv there are some bumps in the curve which correspond to the irregularities in the density of states.
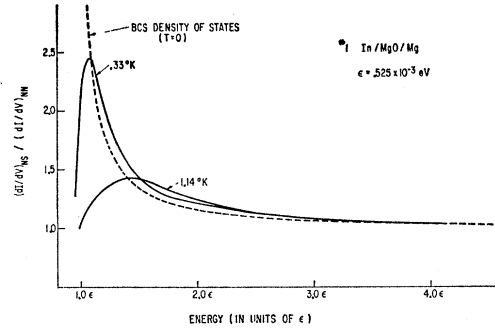

FIG. 12. The relative conductance of an In-MgO-Mg sandwich plotted against energy, for two temperatures. The BCS density of states at $T=0$ is also shown. Note that for maximum detail the zero has been offset.

becomes

$$\frac{d\eta}{dE} = \frac{E}{[E^2 - \epsilon^2(\eta)]^{\frac{1}{2}} + \epsilon(\eta)(\partial/\partial\eta)\epsilon(\eta)}.$$

Swihart[23] has calculated $\epsilon(\eta)$ numerically for an interaction potential which is attractive for $\eta < k\Theta_D$ and repulsive for $\eta > k\Theta_D$, where Θ_D is the Debye temperature. By using his results we obtain a qualitative similarity to our observed curve. This may of course be incidental, because there may be several interaction potentials giving similar results. However, it is interesting to note that the density of states is equal to unity at $\eta \simeq k\Theta_D$.

Figure 11 shows the current-voltage characteristic of a Pb-Pb$_x$O$_y$-Pb sandwich. As seen, we obtain a finite slope at $eV \simeq 2\epsilon$, rather than the jump in current predicted by the Bardeen-Cooper-Schrieffer theory. At applied voltages approximately equal to 6 mv and 11 mv, there are small bumps in the curve corresponding to the irregular density of states.
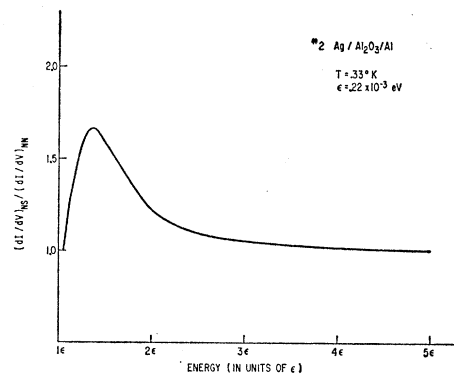

FIG. 13. The relative conductance of an Al-Al$_2$O$_3$-Ag sandwich plotted against energy. The results are similar to those from tin or indium at a higher temperature. Note that for maximum detail the zero has been offset.

[23] J. C. Swihart, IBM J. Research Develop. **6**, 14 (1962).

(c) Indium

In Fig. 12 the density of states obtained for indium is shown. This curve resembles the density of states for tin at a somewhat higher temperature; however, the noise level in this particular case is believed to be rather high. Thus we have more smearing in these experimental curves. Because indium has a low Debye temperature, we have looked for, but not found any irregularities at $eV \simeq k\Theta_D$.

(d). Aluminum

In Fig. 13 the density-of-states curve obtained for aluminum is shown. Because of the low transition temperature of aluminum this curve has a large kT smearing. In Fig. 14 we show the results for two different Al-Al$_2$O$_3$-Al sandwiches which show distinctively different gapwidths. Thus for aluminum, at least, we know that the smearing in the energy gap is probably caused by stress, and thus will not be uniform in one particular sample. The aluminum films in these samples also have different transition temperatures, the thinner films having higher transition temperatures.

In Fig. 15 it is shown that negative resistances are found for Al-Al$_2$O$_3$-Al sandwiches. From these curves we are able to calculate the temperature from Eq. (1)
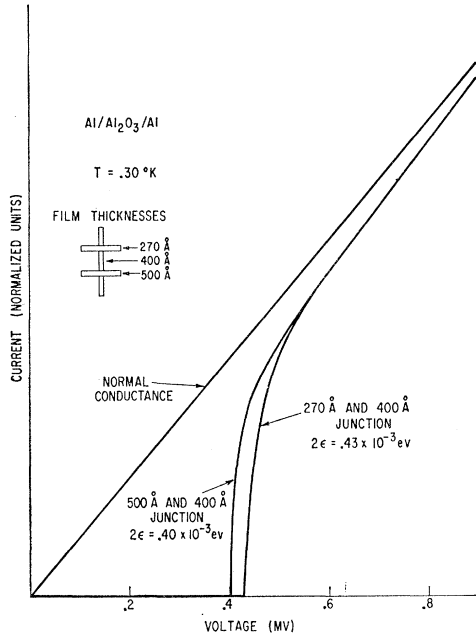

FIG. 14. Current vs voltage curves of two different Al-Al$_2$O$_3$-Al sandwiches showing two distinct energy gaps. The difference in energy gaps is probably due to straining of the aluminum films. Note the absence of the discontinuous current jump at 2ϵ predicted by the BCS theory.
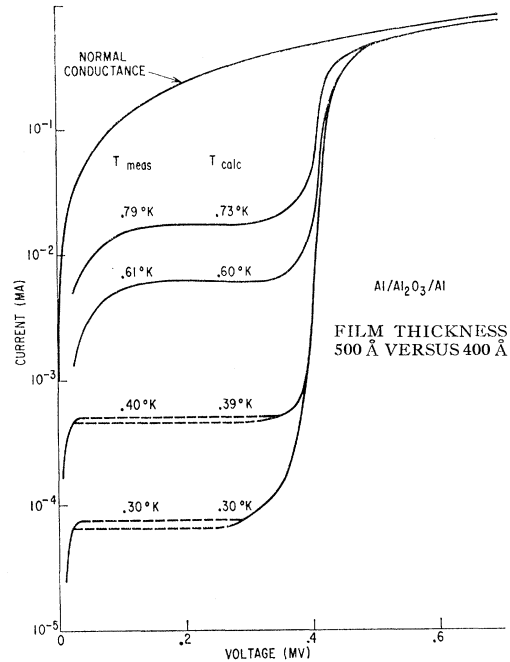

FIG. 15. Current vs voltage curve of an Al-Al$_2$O$_3$-Al sandwich at different temperatures. The current scale is logarithmic. A negative-resistance region is observed. The tunneling current at an applied voltage equal to ϵ is used to calculate the temperature. Measured and calculated temperatures are shown and are in good agreement.

by numerically evaluating the current at $eV = \epsilon$. Our calculations are valid for $\epsilon \gg kT$ only. A very good correlation is found, as seen in Fig. 15.

SUMMARY

The low-temperature experiments all support the Bardeen-Cooper-Schrieffer theory of superconductivity. Some small divergences are found; a smearing in the gap observed by using two superconductors back to back, and some bumps in the density of states for lead. The smearing of the gap, at least in aluminum, is apparently due to stress and might possibly be avoided by using better samples. The bumps in the density of states for lead can be accounted for by using a variable energy gap parameter $\epsilon(\eta)$ which changes sign at $\eta \simeq k\Theta_D$.

ACKNOWLEDGMENTS